Research Article | Vol. 26, No. 24 | 26 Nov 2018 | OPTICS EXPRESS 31075
Optics EXPRESS

150-Gb/s SEFDM IM/DD transmission using log-MAP Viterbi decoding for short reach optical links

BAOXIAN YU,[1,3] CHANGJIAN GUO,[2,3,6] LANGYU YI,[2,3] HAN ZHANG,[4] JIE LIU,[1] XIANHUA DAI,[1,7] ALAN PAK TAO LAU,[5] AND CHAO LU[3]

[1] *School of Electronics and Information Technology, Sun Yat-sen University, Guangzhou 510006, China*
[2] *South China Academy of Advanced Optoelectronics, South China Normal University, Guangzhou 510006, China*
[3] *Photonics Research Center, Department of Electronic and Information Engineering, The Hong Kong Polytechnic University, Hong Kong, China*
[4] *School of Physics and Telecommunication Engineering, South China Normal University, Guangzhou 510006, China*
[5] *Photonics Research Center, Department of Electrical Engineering, The Hong Kong Polytechnic University, Hong Kong, China*
[6] *changjian.guo@coer-scnu.org*
[7] *issdxh@mail.sysu.edu.cn*

Abstract: Spectral efficient frequency division multiplexing (SEFDM) can improve the spectral efficiency for next-generation optical and wireless communications. In this work, we apply SEFDM in beyond 100-Gb/s optical intensity modulation and direct detection transmissions and propose a low-complexity logarithmic-maximum-a-posteriori (log-MAP) Viterbi decoding algorithm to achieve the maximum likelihood (ML) detection. We evaluate the likelihood of detections using a posteriori probability instead of Euclidean distance by taking both noise and inter-carrier interference into consideration. In order to balance the performance and complexity, we then employ Viterbi decoding principle to retain only certain paths with ML detections (a.k.a., the surviving paths) while discarding the others during the decoding procedure. Results show that the proposed log-MAP Viterbi decoding scheme achieves optimal performance due to the precise likelihood evaluation, which guarantees the retention of the global ML detection. By using the proposed decoding scheme, the data rate of SEFDM signals can reach 150-Gb/s in a 2-km standard single mode fiber transmission, using only 28-GHz bandwidth and 16-QAM modulation. Experimental results show that the 16-QAM modulated SEFDM signal with a bandwidth compression factor of 0.8 outperforms 32-QAM modulated OFDM, while both signals have the same bandwidth (28-GHz) and data rate (140-Gb/s), which demonstrate the superiority of SEFDM in optical short reach applications.

1. Introduction

Driven by the emerging applications such as Internet of Things, big data, cloud computing, etc., the ever-increasing demand for high speed in data centers requires short reach optical systems that operates beyond 100-Gb/s. Recently, it has been reported that the short reach interconnects will face severe internet traffic in the future [1]. In short reach applications, intensity modulation and direct detection (IM/DD) is preferred over coherent schemes owing to its simple implementation and low cost. Conventional schemes achieving the high data rate short reach transmissions include single carrier pulse amplitude modulation (PAM), discrete multi-tone (DMT), carrier-less amplitude and phase modulation (CAP), as well as faster than Nyquist (FTN) signaling [2–8].

Spectrally efficient frequency division multiplexing (SEFDM) is another effective scheme to improve the spectral efficiency (SE), through compressing sub-carriers closer than orthogonal

#339841 https://doi.org/10.1364/OE.26.031075
Journal © 2018 Received 17 Jul 2018; revised 16 Oct 2018; accepted 16 Oct 2018; published 12 Nov 2018

Optics EXPRESS

frequency division multiplexing (OFDM). Consequently, the orthogonality between sub-carriers is deliberately violated, leading to inter-carrier interference (ICI), which may pose challenges in detection [9]. Many efforts have been made to pursue a favorable trade-offs between performance and complexity [9–11]. In [9], sphere decoding (SD) was employed to achieve the maximum likelihood (ML) detection but suffers from tremendous computational burden in the cases of large symbol-size, small bandwidth compression factor (BCF), and high noise level. Iterative detection (ID) with soft decision entails much less computations, yet it may encounter an error floor even when a moderate amount of ICI exists [10]. Recently, we proposed a precondition-aided decision feedback approach to achieve an attractive balance between the performance and the complexity with a limitation of small constellation [11]. Thanks to the above detection schemes, SEFDM has been widely considered in short reach optical fiber communications [12–14], In 2014, SEFDM was first experimentally applied in IM/DD systems, achieving 25% bandwidth gain in comparison with OFDM [12]. 20-Gb/s and 98.7-Gb/s SEFDM IM/DD transmissions have been successfully demonstrated using cascaded BPSK ID fixed-complexity SD (CBID-FSD) [13] and enhanced ID (EID) [14], respectively. In addition, SEFDM can simultaneously enjoy higher SE and a diversity gain in chromatic dispersive channel, which indicates the superiority of SEFDM in long reach links [15].

In this work, we investigate beyond 100-Gb/s short reach optical links based on SEFDM and propose a low-complexity logarithmic-maximum-a-posteriori (log-MAP) Viterbi decoding algorithm to achieve the maximum likelihood (ML) detection for SEFDM. We first elaborate the decoding principle and then verify its effectiveness by both simulation and experiment. Results show that the proposed log-MAP Viterbi decoding method outperforms existing schemes, such as CBID-FSD. Using the proposed detection method, a 150-Gb/s SEFDM IM/DD transmission over 2-km of standard single mode fiber (SSMF) is successfully demonstrated. Particularly, in the case of 28-GHz bandwidth and 140-Gb/s data rate, 16-QAM modulated SEFDM signal with a BCF of 0.8 performs better than 32-QAM modulated OFDM, which indicates the superiority of SEFDM IM/DD transmissions in comparison with conventional OFDM ones.

2. Operating principle

2.1. SEFDM system

SEFDM is essentially a multi-carrier technology, where the baseband signal is given by

$$x(t) = \sum_{k=0}^{N-1} S_k \exp(j2\pi k\Delta f t), \tag{1}$$

where S_k is symbol modulated on k^{th} sub-carrier, Δf and N denote sub-carriers' spacing and symbol-size, respectively. Discretize $x(t)$ in Eq. (1) by N_1 samples in symbol duration T, we have

$$x_n := x\left(\frac{nT}{N_1}\right) = \sum_{k=0}^{N-1} S_k \exp\left(\frac{j2\pi\alpha kn}{N_1}\right), n = 0, 1, \cdots, N_1 - 1, \tag{2}$$

where $\alpha = \Delta f T$ represents the BCF. In conventional orthogonal systems, a.k.a., OFDM, we have $\alpha = 1$, while $\alpha < 1$ in the case of SEFDM. To be specific, SEFDM saves either the occupied bandwidth or the symbol duration to achieve a higher SE. Take $\alpha = 0.8$ as an example, SEFDM yields a 25% spectral gain in comparison with OFDM.

Analogous to OFDM, the typical SEFDM transceiver is based on inverse fast Fourier transform (IFFT) and fast Fourier transform (FFT). As illustrated in the previous literature [11], assuming

Optics EXPRESS

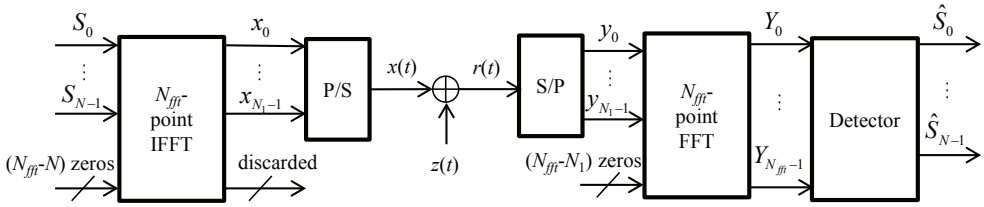

Fig. 1. SEFDM transceiver diagram using IFFT method.

that $N_{fft} = \frac{N_1}{\alpha}$ is an integer, we can rewrite Eq. (2) as

$$x_n = \sum_{k=0}^{N_{fft}-1} S'_k \exp\left(\frac{j2\pi kn}{N_{fft}}\right), n = 0, 1, \cdots, N_1 - 1, \tag{3}$$

where $S'_k = S_k$ for $k < N$, otherwise $S'_k = 0$. In another word, IFFT is implemented after padding $N_{fft} - N$ zeros at the end of each SEFDM block, and only the first N_1 IFFT samples are transmitted. Similarly, to implement N_{fft}-point FFT at the receiver, we pad $N_{fft} - N_1$ zeros after each SEFDM block with N_1 samples. The transceiver principle of SEFDM in additive white Gaussian noise (AWGN) channel is depicted Fig. 1.

After FFT, as shown in Fig. 1, the received signal can be written by

$$Y_k = W_{k,k}S_k + \sum_{i=0, i\neq k}^{N-1} W_{k,i}S_i + Z_k, \tag{4}$$

where Z_k denotes zero-mean AWGN with a variance of σ^2 and

$$W_{k,i} = \frac{1}{N_{fft}} \sum_{n=0}^{N_1-1} \exp\left(\frac{-j2\pi n(k-i)}{N_{fft}}\right). \tag{5}$$

The first and second items on right-hand-side of Eq. (4) are the desired symbol and ICI, respectively. ICI may result in either an error floor or additional computational burden in detection. To address this issue, we propose a log-MAP Viterbi decoding algorithm in this work, where the detailed principle is elaborated as follows.

2.2. Log-MAP Viterbi decoding algorithm

Consider the joint detection of the first P symbols in sequential decoding, the residual interference including ICI resulted from the following undetected symbols and noise on k^{th} sub-carrier reads

$$\gamma_k = \sum_{i=P}^{N-1} W_{k,i}S_i + Z_k, k = 0, 1, \cdots, P - 1, \tag{6}$$

Without loss of generality, suppose that the transmitted symbols are independent identically distributed with unit power, i.e., $E\{|S_k|^2\} = 1$ and $E\{|S_k S_i^*|\} = 0, \forall k \neq i$. We therefore have $E\{\gamma_k\} = 0$ and the covariance of the interference γ_k reads

$$\Gamma_{k,l} = E\{\gamma_k^* \gamma_l\} = \sum_{i=P}^{N-1} \sum_{j=P}^{N-1} W_{k,i}W_{j,l} + A_{k,l}, \tag{7}$$

Optics EXPRESS

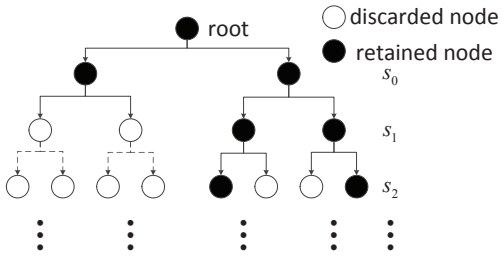

Fig. 2. Tree diagram of the proposed log-MAP Viterbi decoding algorithm. The solid dots denote the retained ML detections, while the others denote the discarded ones.

where

$$A_{k,l} = \begin{cases} \sigma^2 & k = l \\ 0 & k \neq l \end{cases}.$$

According to the central limit theorem, the interference $\gamma_k, k = 0, 1, \cdots, P-1$ in Eq. (6) obey P-demensional zero-mean joint Gaussian distribution with a covariance matrix $\mathbf{\Gamma}$, where $\Gamma_{k,l}$ denotes its $\{k, l\}$-entry. Therefore, the logarithmic-a-posteriori-probability (log-APP) of the joint detection on $S_k, k = 0, 1, \cdots, P-1$ is given by

$$P = -\mathbf{d}^{\mathrm{H}}\mathbf{\Gamma}^{-1}\mathbf{d}, \tag{8}$$

where $(\cdot)^{\mathrm{H}}$ denotes Hermitian transpose and $\mathbf{d}$ is a $P \times 1$ vector with k^{th}-entry written as

$$d_k = Y_k - \sum_{i=0}^{P-1} W_{k,i} S_i, \tag{9}$$

As stated above, taking both noise and residual ICI into consideration, log-APP performs precise likelihood evaluation on detections. In this work, we propose log-MAP Viterbi decoding scheme, where C is set as the number of surviving paths in Viterbi decoding. During the sequential decoding, i.e., for each P from 0 to $N-1$, we retain C ML detections with maximum log-APP and discard the others. The decoding procedure can be interpreted using a tree diagram by taking BPSK and $C = 2$ as an example, as shown in Fig. 2. In each step of decoding (corresponding to each row of tree diagram in Fig. 2), we retain 2 ML detections (corresponding to solid dots of tree diagram in Fig. 2) from 4 detection candidates (corresponding to dots connected with solid lines of tree diagram in Fig. 2).

Simulation results in Fig. 3 demonstrate the superiority of the proposed log-MAP Viterbi decoding algorithm. The parameters used in simulations are listed in Table 1. Figure 3(a) shows the bit error rate (BER) performance of the proposed log-MAP Viterbi decoding algorithm for SEFDM with $\alpha = 0.80$ at various numbers of surviving paths C. For reference, we also perform SD [9] at $N = 16$ and the same BCF (SD is infeasible due to its prohibitive complexity in the cases of large symbol size, such as $N = 80$). We can see from Fig. 3(a) that larger C yields better BER performance since it guarantees higher probability to retain the global ML detection. In addition, the performance of the proposed algorithm saturates with that of SD (i.e., ML performance) at $C = 4$ and $C = 16$ for 4-QAM and 16-QAM, respectively, which indicates the ML performance achieving capability as well as the low complexity of the proposed method (note that the proposed method can also perform with higher order modulation formats, such as 64-QAM). This fact is attributed to the precise likelihood evaluation on detections using log-APP by taking both noise and residual ICI into consideration. We then examine the effectiveness of the proposed log-MAP

Optics EXPRESS

Table 1. Parameters used for experiments and simulations

Items	Values
Symbol-size	$N = 80$
FFT size	$N_{fft} = 256$
Transmitted samples	$N_1 = 192, 204, 224$
Corresponding BCF	$\alpha = 0.75, 0.80, 0.88$
Guard interval length	16
Modulation formats	4-QAM, 16-QAM, 32-QAM
signal used	SEFDM, OFDM
Fiber length	2-km

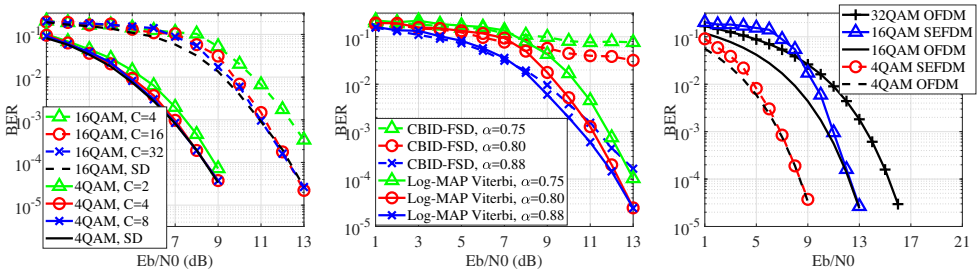

Fig. 3. (a) Simulated BER performance of the proposed log-MAP Viterbi decoding algorithm with various values of C for SEFDM with $\alpha = 0.80$ using 4-QAM and 16-QAM modulations in AWGN channel; (b) comparison between the proposed log-MAP Viterbi decoding scheme with conventional CBID-FSD for SEFDM with various values of α; (c) comparison of performance between SEFDM with OFDM.

Viterbi decoding algorithm by comparing with CBID-FSD. For feasibility of CBID-FSD, we reduce N, N_{fft}, N_1 by half (FSD is also infeasible in the cases of large symbol size). We can learn from Fig. 3(b) that our proposed scheme outperforms CBID-FSD with the same C (i.e., costing comparable computations) at various BCFs. Besides, the proposed algorithm is much more robust to BCF, while CBID-FSD suffers from severe performance degradation in the cases of small α. Figure 3(c) compares the performance between OFDM and SEFDM with $\alpha = 0.80$. As shown in Fig. 3(c), SEFDM achieves a spectral gain of 25% in comparison with OFDM at a price of performance degradation in low signal-to-noise-ratio (SNR) scenarios for both 4-QAM and 16-QAM. Nevertheless, this penalty vanishes as SNR grows. For fairness of comparison, we consider 16-QAM SEFDM with $\alpha = 0.80$ and 32-QAM OFDM since both achieve a SE of 5-bps/Hz. As illustrated in Fig. 3(c), the former performs comparably with the latter in the case of high noise level, and yields a significant performance improvement in high SNR scenarios, which infers the superiority of SEFDM.

Finally, we evaluate the complexity of the proposed log-MAP Viterbi decoding scheme. In each step of decoding , we evaluate the likelihood of CM detections (corresponding to dots connected with solid lines in the same row of tree diagram in Fig. 2), and sequential detection performs

Optics EXPRESS

Table 2. General computational complexity comparison

Method	Complexity order	Remarks
log-MAP Viterbi	$O(CNM)$	linear order of N and M
SD	$O(M^{\theta N})$ [10]	$\theta \to 1$ in low SNR or small BCF cases
MLSE	$O(NM^L)$ [18]	Large L in small BCF cases

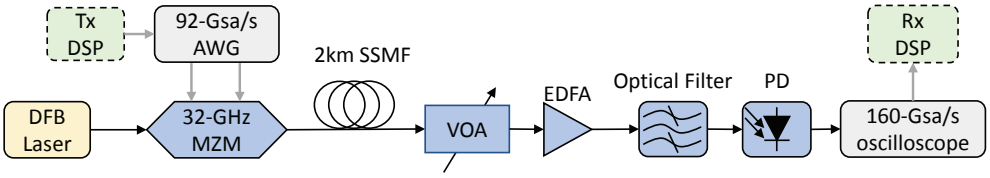

Fig. 4. Experimental setup.

N steps in total. Therefore, the proposed method is feasible since its general complexity is in the order of $O(CNM)$. We validate the low complexity of the proposed method by comparing SD and ML sequence estimation (MLSE) as references since SD achieves the ML performance and has been regarded as a benchmark in related works, and MLSE is a mature technique that has been applied to high speed implementation [16]. The complexity comparison among these methods is summarized in Table 2, where $0 < \theta < 1$ depends on noise level [17], and $L > 1$ is an integer denoting the number of filter taps of MLSE. We can learn from Table 2 that the proposed log-MAP Viterbi decoding scheme entails the least computations since its complexity is merely in a linear order of constellation cardinality and symbol-size, while SD and MLSE suffer from exponential complexity increment in the case of large M and N. In addition, according to the results in Fig. 3, the proposed method with $C = M$ can yield the saturate performance close to the ML one. In this case, the proposed method entails an equivalent complexity in the order of $O(NM^2)$, which is comparable to the minimum complexity of MLSE (i.e., $L = 2$). This fact indicates the feasibility of the proposed log-MAP Viterbi decoding scheme for high speed implementation.

3. Experimental setup

The experiment setup and parameters are shown in Fig. 4 and Table 1, respectively. The SEFDM signal was generated offline by MATLAB using IFFT in Eq. (3). In order to generate the real-valued DMT signal, data were modulated on $2^{\text{nd}} - 81^{\text{st}}$ sub-carriers and mapped conjugate symmetrically into $177^{\text{th}} - 256^{\text{th}}$ ones, while the other sub-carriers were zero padded. After IFFT, the last $N_{fft} - N_1$ samples in time-domain were discarded to form the SEFDM signal, which was then padded with 16-point zero-valued guard interval (GI) to mitigate inter-block interference. After parallel/serial (P/S) conversion, the SEFDM signals, following one block of timing synchronization pattern and 128 blocks of OFDM training sequences, were loaded into an arbitrary waveform generator (AWG) operating at f_s = 90-Gsa/s. Due to the limited bandwidth of AWG, the overall bandwidth of our experimental setup is about 30-GHz. To ensure a satisfactory performance, we used 80 sub-carriers to load data, and thereby, the occupied bandwidth was $B = f_s \frac{N}{N_{fft}}$ = 28.125-GHz. The output signal from the AWG was amplified and then sent to a Mach Zehnder modulator (MZM) for double side-band (DSB) modulation. The optical carrier

Optics EXPRESS

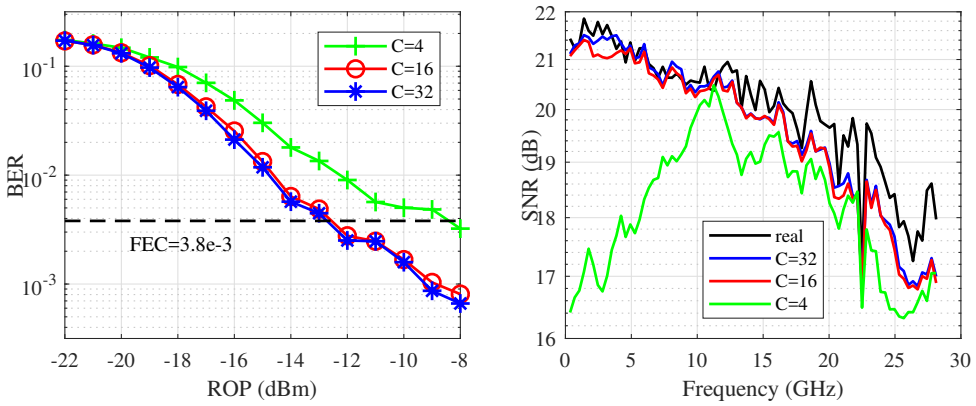

(a) (b)

Fig. 5. (a) BER performance of the proposed log-MAP Viterbi decoding algorithm with various values of C for SEFDM with $\alpha = 0.80$ using 16-QAM modulation after 2-km SSMF transmission; (b) calculated SNR after ICI cancellation using the proposed decoding scheme, compared with the real SNR obtained via OFDM training.

used in this experiment had a center wavelength of 1550.12-nm. After 2-km SSMF transmission, a variable optical attenuator (VOA) was used to adjust the received optical power (ROP) before an Erbium doped fiber amplifier (EDFA) with a noise figure of about 4.3-dB. The optical signals were filtered and then detected by a photo detector (PD) with a bandwidth of 43-GHz. The electrical signals after PD were digitized by a 160-Gsa/s real time oscilloscope and then processed off-line. The main off-line DSP procedures include timing synchronization, serial/parallel (S/P) conversion, GI processing followed by DFT, channel estimation and equalization, as well as data detection using the proposed log-MAP Viterbi decoding algorithm.

4. Results and discussion

We first conducted an experiment to validate the effectiveness of the proposed log-MAP Viterbi decoding algorithm. In this experiment, BCF $\alpha = 0.80$ and 2-km SSMF were considered. As shown in Fig. 5(a), lager number of surviving paths C yields better performance, which agrees with the analysis and simulation results in Section 2. To be specific, $C = 16$ outperforms $C = 4$ by a ROP improvement of 4dBm at FEC limit (BER = 3.8e-3) and the performance of the proposed log-MAP Viterbi decoding algorithm saturates at $C = 16$, which indicates the low complexity. Figure 5(b) illustrates SNR after ICI cancellation using the proposed decoding scheme, i.e., eliminate the second item on right-hand-side of Eq. (4) using the detected results. We can learn from Fig. 5(b) that SNR of $C = 16$ and $C = 32$ are very close to the real one, while the SNR gap between $C = 4$ and the real one is significant, especially in low frequency band. This is reasonable because in sequential decoding, the data modulated in the sub-carriers of low frequency is first detected with entire ICI. Therefore, the global ML detections might rank behind due to the small log-APP (mainly infected by the unexpected ICI), and might be discarded if C is not large enough, which leads to severe SNR degradation at low frequency. As the sequential decoding goes on, the residual ICI is limited, and thus, the calculated SNR is improved, and the gap with the real SNR becomes relatively stable.

Figure 6 depicts the signal distribution before and after ICI cancellation using the proposed log-MAP Viterbi decoding algorithm. Signals are indistinguishable before data detection due to the self-introduced ICI, while the detected ones are discernible, which indicates the capability of

Optics EXPRESS

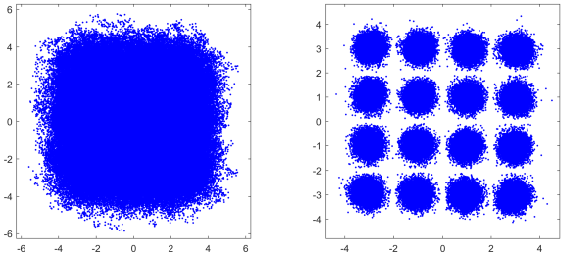

(a) (b)

Fig. 6. Received signal distributions of SEFDM before (left) and after (right) ICI cancellation using the proposed log-MAP Viterbi decoding algorithm.

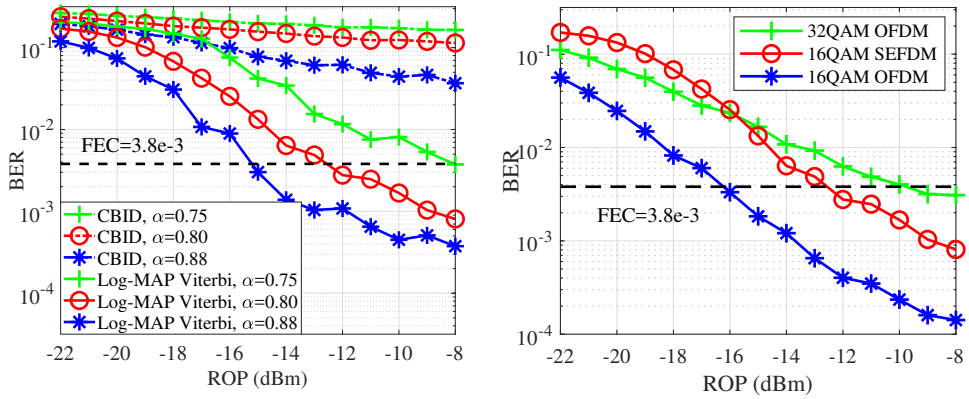

(a) (b)

Fig. 7. (a) BER performance of the proposed log-MAP Viterbi decoding algorithm with $C = 16$ for SEFDM with various values of α using 16-QAM modulations after 2-km SSMF transmission, compared with CBID; (b) BER comparison between OFDM and SEFDM with $\alpha = 0.80$ after 2-km SSMF transmission.

ICI cancellation of the proposed decoding scheme.

Finally, we demonstrated the performance of the 16-QAM SEFDM signals with various BCFs after 2-km SSMF transmission using our proposed log-MAP Viterbi decoding scheme, in comparison with 16-QAM and 32-QAM modulated OFDM signals using the same bandwidth (28-GHz). We can learn from the results shown in Fig. 7(a) that, the proposed decoding scheme outperforms conventional CBID (SD-based methods fail to work at $N = 80$ because of the excessive computations, and thus, no numerical results of SD and FSD are displayed). In addition, the proposed decoding scheme performs better in the cases of larger BCF due to less ICI. Nevertheless, by using the proposed decoding algorithm, BER performance of SEFDM with α reaches FEC limit, achieving a spectral gain of 33.3% and a data rate of 150-Gb/s. To yield a SE of 5-bps/Hz, as shown in Fig. 7(b), 16-QAM SEFDM with $\alpha = 0.80$ requires a ROP penalty of 3.1-dBm at FEC limit in comparison with 16-QAM OFDM. For fairness of comparison, we also conducted an experiment using 32-QAM OFDM, which also achieve the same SE. we can see from Fig. 7(b) that 16-QAM SEFDM outperforms 32-QAM OFDM by a ROP gain of 2.8-dBm at FEC limit, which indicates the superiority of SEFDM to achieve higher SE.

Optics EXPRESS

5. Conclusions

We have experimentally demonstrated beyond 100-Gb/s optical IM/DD transmissions using SEFDM to achieve higher SE. To mitigate the self-introduced ICI, we have proposed a low-complexity log-MAP Viterbi decoding scheme for data detection. Compared with conventional methods, the proposed algorithm takes both ICI and noise into consideration and use log-APP instead of Euclidean distance to evaluate the likelihood of detections. Simulation and experimental results showed that the proposed log-MAP Viterbi algorithm achieves ML performance due to the precise evaluation on detection candidates. By using the proposed detection scheme, a 150-Gb/s SEFDM IM/DD transmission over 2-km SSMF has been successfully demonstrated, achieving a spectral gain of up to 33.3% in comparison with OFDM, as well as an SE of 5.33-bps/Hz by merely using 16-QAM. In addition, under the same SE of 5-bps/Hz, 16-QAM modulated SEFDM with a BCF of 0.8 outperforms 32-QAM modulated OFDM, which indicates the superiority of SFEDM in short-reach applications.

Funding

National Natural Science Foundation of China (NSFC) (61435006, 61872396, 61471176, 61471175); Natural Science Foundation (NSF) of Guangdong Province (2014A030308014); Hong Kong Government General Research Fund (PolyU 152079/14E); Pearl River Science and Technology Nova Program of Guangzhou (201710010028, 201610010199); Guangdong Province Outstanding Young Teacher Training Program (YQ2015046); Science and Technology Planning Project of Guangdong Province (2017A010101015, 2017B030308009, 2017KZ010101); Special Project for Youth Top-notch Scholars of Guangdong Province (2016TQ03X100).

References

1. K. Zhong, X. Zhou, J. Huo, C. Yu, C. Lu, and A. P. T. Lau, "Digital signal processing for short-reach optical communications: a review of current technologies and future trends," J. Light. Technol. **36**, 377–400 (2018).
2. M. Chagnon, S. Lessard, and D. V. Plant, "336 Gb/s in direct detection below KP4 FEC threshold for intra data center applications," IEEE Photon. Technol. Lett. **28**, 2233–2236 (2016).
3. Y. Zheng, J. Zhang, X. Hong, and C. Guo, "Generation and detection of 170.49-Gb/s single polarization IM/DD optical OFDM signals enabled by Volterra nonlinear equalization," in *Asia Communications and Photonics Conference,* (Optical Society of America, 2016), pp. ATh2D–1.
4. S. Kanazawa, H. Yamazaki, Y. Nakanishi, T. Fujisawa, K. Takahata, Y. Ueda, W. Kobayashi, Y. Muramoto, H. Ishii, and H. Sanjoh, "Transmission of 214-Gbit/s 4-PAM signal using an ultra-broadband lumped-electrode EADFB laser module," in *Optical Fiber Communication Conference,* (Optical Society of America, 2016), pp. Th5B–3.
5. M. I. Olmedo, T. Zuo, J. B. Jensen, Q. Zhong, X. Xu, S. Popov, and I. T. Monroy, "Multiband carrierless amplitude phase modulation for high capacity optical data links," J. Light. Technol. **32**, 798–804 (2014).
6. X. Zhou, K. Zhong, J. Huo, J. Yuan, F. Li, L. Wang, K. Long, A. P. T. Lau, and C. Lu, "Polarization-multiplexed DMT with IM-DD using 2× 2 MIMO processing based on SOP estimation and MPBI elimination," IEEE Photon. J. **7**, 1–12 (2015).
7. K. Zhong, X. Zhou, Y. Gao, W. Chen, J. Man, L. Zeng, A. P. T. Lau, and C. Lu, "140 Gbit/s 20km transmission of PAM-4 signal at 1.3 μm for short reach communications," IEEE Photon. Technol. Lett. **27**, 1757–1760 (2015).
8. K. Zhong, X. Zhou, Y. Wang, L. Wang, J. Yuan, C. Yu, A. P. T. Lau, and C. Lu, "Experimental demonstration of 608Gbit/s short reach transmission employing half-cycle 16QAM Nyquist-SCM signal and direct detection with 25Gbps EML," Opt. Express **24**, 25057–25067 (2016).
9. I. Kanaras, A. Chorti, M. R. Rodrigues, and I. Darwazeh, "Spectrally efficient FDM signals: bandwidth gain at the expense of receiver complexity," in *Communications, 2009. ICC'09. IEEE International Conference on,* (IEEE, 2009), pp. 1–6.
10. S. J. Heydari, M. F. Naeiny, and F. Marvasti, "Iterative detection with soft decision in spectrally efficient FDM systems," arXiv preprint arXiv:1304.4003 (2013).
11. B. Yu, H. Zhang, and X. Dai, "A low-complexity demodulation technique for spectrally efficient FDM systems using decision-feedback," IET Commun. **11**, 2386–2392 (2017).
12. I. Darwazeh, T. Xu, T. Gui, Y. Bao, and Z. Li, "Optical SEFDM system; bandwidth saving using non-orthogonal sub-carriers," IEEE Photon. Technol. Lett. **26**, 352–355 (2014).
13. J. Huang, Q. Sui, Z. Li, and F. Ji, "Experimental Demonstration of 16-QAM DD-SEFDM with cascaded BPSK iterative detection," IEEE Photon. J. **8**, 1–9 (2016).

Optics EXPRESS

14. C. Guo, B. Yu, L. Yi, Y. Xu, X. Wu, J. Liu, and H. Zhang, "98.7-Gb/s optical SE-DMT transmission using an enhanced decision-directed algorithm with preconditions," in *Asia Communications and Photonics Conference,* (Optical Society of America, 2017), pp. S4B–2.
15. B. Yu, L. Yi, C. Guo, J. Liu, X. Dai, A. Lau, and C. Lu, "Dispersion Tolerant 66.7-Gb/s SEFDM IM/DD Transmission over 77-km SSMF," in *Optical Communication (ECOC), 2018 European Conference on,* (IEEE, 2018), pp. We2.25–1.
16. Z. Zhang, C. Li, J. Chen, T. Ding, Y. Wang, H. Xiang, Z. Xiao, L. Li, M. Si, and X. Cui, "Coherent transceiver operating at 61-gbaud/s," Opt. Express **23**, 18988–18995 (2015).
17. B. Hassibi and H. Vikalo, "On the sphere-decoding algorithm i. expected complexity," IEEE Trans. on Signal Process. **53**, 2806–2818 (2005).
18. H. C. Myburgh and J. C. Olivier, "Low complexity mlse equalization in highly dispersive rayleigh fading channels," EURASIP J. on Adv. Signal Process. **2010**, 10 (2010).